Efficient Localization of Synchronous EEG Source Activities Using a Modified RAP-MUSIC Algorithm

Hesheng Liu, *Member, IEEE,* and Paul H. Schimpf*, *Member, IEEE*

***Abstract*—Synchronization across different brain regions is suggested to be a possible mechanism for functional integration. Noninvasive analysis of the synchronization among cortical areas is possible if the electrical sources can be estimated by solving the electroencephalography inverse problem. Among various inverse algorithms, spatio-temporal dipole fitting methods such as RAP-MUSIC and R-MUSIC have demonstrated superior ability in the localization of a restricted number of independent sources, and also have the ability to reliably reproduce temporal waveforms. However, these algorithms experience difficulty in reconstructing multiple correlated sources. Accurate reconstruction of correlated brain activities is critical in synchronization analysis. In this study, we modified the well-known inverse algorithm RAP-MUSIC to a multistage process which analyzes the correlation of candidate sources and searches for independent topographies (ITs) among precorrelated groups. Comparative studies were carried out on both simulated data and clinical seizure data. The results demonstrated superior performance with the modified algorithm compared to the original RAP-MUSIC in recovering synchronous sources and localizing the epileptiform activity. The modified RAP-MUSIC algorithm, thus, has potential in neurological applications involving significant synchronous brain activities.**

***Index Terms*—EEG, Inverse problem, RAP-MUSIC, synchronization.**

I. Introduction

EXTENSIVE studies have suggested that synchronization is a possible mechanism for neural integration and could play a crucial role in brain function [1]–[4]. Synchronized activities exist not only within local brain regions but also across areas far apart in the brain [5]. To understand the brain network, functional imaging techniques such as functional magnetic resonance imaging (fMRI) and positron emission tomography (PET) are widely used. However, synchrony between associated brain areas is usually transient and may emerge and disappear in a short time [6]. fMRI and PET are not able to fully reveal this transient activity due to their poor temporal resolution. An alternative tool is electroencephalography (EEG), which can provide a temporal resolution in milliseconds. Currently most synchronization studies are based on scalp EEG. Because of volume conduction a single electrical source in the cortex may produce synchronized signals on several scalp channels. Analyzing the synchrony of scalp EEG could, thus, be misleading because the synchronized components may come from the same source [7]. A way to improve the spatial resolution of EEG is the inverse method, which attempts to reconstruct brain sources from scalp measurements. Solution of the EEG inverse problem benefits from a head model which correctly reflects the relationship between neural current sources and measurements. Both spherical head models and, more recently, realistic-geometry head models have been used. The disadvantage of EEG is that the signals from multiple sources are mixed as they propagate through the inhomogeneous tissues surrounding the brain. An alternative to EEG is magnetoencephalography (MEG), which is less affected by inhomogeneities and the high impedance of skull. However, MEG is insensitive to deep or radially oriented sources. Since EEG and MEG provide complementary information on the sources, a better solution may be achieved by combining these two measurements. The inverse algorithm will be discussed in this paper is applicable to both EEG and MEG signals. The EEG/MEG inverse problem is known to be ill-posed and requires *a priori* assumptions regarding the source model to achieve a unique solution. These assumptions are highly application-specific. Many source models are possible, such as a single dipole model, multidipole model and distributed current source model. Various inverse methods have been proposed based on different models. Reviews of these models and methods can be found in [8], [9]. Among current inverse algorithms, some can be classified as spatio-temporal methods. Prominent examples are dipole fitting algorithms such as R-MUSIC [10] and RAP-MUSIC [11]. They separate the EEG signal into multiple components according to temporal characteristics, and then localize the sources for each component. These methods can recover independent or weakly correlated sources very well. However, both methods have difficulty in separating highly correlated sources and can, thus, produce large localization errors when such sources are present.

Other algorithms use a spatial-only approach. These methods process the EEG signals one time-sample at a time and optimize the source distribution to fit the measurements at the given time sample. Examples are weighted minimum norm (WMN) [12], LORETA [13], [14], sLORETA [15], and FOCUSS [16]. These spatial inverse methods are not influenced by the temporal course of the sources and, thus, their performance is not significantly degraded by source correlation. However, by processing only a single time sample, such methods usually have higher localization errors on independent sources in the presence of noise. Spatial-only inverse methods may also deform the source waves when continuous EEG

Manuscript received January 26, 2005; revised August 5, 2005. This work was supported in part by the National Science Foundation (NSF) under Grant 0112742. *Asterisk indicates corresponding author.*

H. Liu is with the School of Electrical Engineering and Computer Science, Washington State University, Spokane, WA 99202 USA (e-mail: heshengliu@yahoo.com).

*P. Schimpf is with the School of Electrical Engineering and Computer Science, Washington State University, Spokane, WA 99202 USA (e-mail: schimpf@wsu.edu).

Digital Object Identifier 10.1109/TBME.2006.870236

recordings are processed. Low-resolution methods such as WMN, LORETA, and sLORETA will mix the waveforms of sources that fall within their wide point-spread functions. High-resolution methods such as FOCUSS and L1-norm [17] usually produce discontinuous waveforms because of their nonlinearity. Incorrect temporal waveforms will preclude subsequent synchronization analysis.

In the human brain, interaction among brain sources can be highly complex. Correlations at all levels may exist, including perfect synchronization. In the rest of this paper, highly correlated sources are referred to as synchronous sources, as in [10]. A method which fails to handle synchronous sources will produce incorrect source distributions, resulting in incorrect conclusions regarding the interaction between different brain regions.

Efforts have been made to enable spatio-temporal methods to process highly correlated sources. R-MUSIC and RAP-MUSIC introduced the important concept of independent topographies (ITs). Instead of representing dipoles individually, an IT is comprised of one or more nonrotating dipoles with perfectly correlated time courses. Because a multidipole IT is comprised of multiple synchronous sources, the IT model provides the potential for localizing synchronous sources. However, searching for such sources is far from straightforward. These algorithms begin by first searching for a single-dipole IT to fit a specific component of the signal. If the correlation between the signal component and the best-fit single dipole IT falls below a preset threshold, a multidimensional search for an IT containing multiple synchronous dipoles is performed. There are two problems that are not explicitly addressed by R-MUSIC and RAP-MUSIC. 1) How to establish a correlation threshold for scanning multisource ITs. In [10], the authors simply suggest a correlation threshold of 95%. However, an appropriate correlation threshold is highly dependent on the signal-to-noise ratio (SNR), as shown in [18] and demonstrated further here. 2) How to deal with the factorial increasing computational complexity when multiple synchronous sources are present. The head model usually contains thousands of nodes that are candidate source locations. Thus, even two synchronous sources will incur an exhaustive search among over one million possible combinations of these nodes. This complexity can be mediated, to some extent, by initially searching over a reduced solution as demonstrated in [10] and again in [18], but this strategy cannot keep up with the factorial complexity of multiple sources. It is also possible to search for synchronous sources using nonlinear methods; however, they usually find local optima rather than the global solution. A global search for more than two synchronous sources is practically impossible though synchrony over multiple brain regions is common.

This paper introduces a modified version of RAP-MUSIC that attempts to integrate the spatio-temporal and spatial-only approaches in a way that preserves both of their advantages. Special attention will be paid to highly correlated sources. For simplicity of presentation, this modified RAP-MUSIC algorithm is referred to as precorrelated and orthogonally projected MUSIC (POP-MUSIC).[1]

[1]Code to implement POP-MUSIC is available upon request to the corresponding author.

II. Method

A. IT Source Model and RAP-MUSIC

For a generalized problem with p current dipoles in the brain and m electrodes on the scalp, the spatio-temporal form of the EEG forward problem can be expressed as

$$\underset{m\times n}{\begin{bmatrix} v(\mathbf{r}_1,t_1) & \cdots & v(\mathbf{r}_1,t_n) \\ \vdots & \ddots & \vdots \\ v(\mathbf{r}_m,t_1) & \cdots & v(\mathbf{r}_m,t_n) \end{bmatrix}} = \underset{m\times 3p}{\begin{bmatrix} \mathbf{G}(\mathbf{r}_1,\mathbf{l}_1) & \cdots & \mathbf{G}(\mathbf{r}_1,\mathbf{l}_p) \\ \vdots & \ddots & \vdots \\ \mathbf{G}(\mathbf{r}_m,\mathbf{l}_1) & \cdots & \mathbf{G}(\mathbf{r}_m,\mathbf{l}_p) \end{bmatrix}} \times \underset{3p\times n}{\begin{bmatrix} \mathbf{s}_1(t_1) & \cdots & \mathbf{s}_1(t_n) \\ \vdots & \ddots & \vdots \\ \mathbf{s}_p(t_1) & \cdots & \mathbf{s}_p(t_n) \end{bmatrix}} \quad (1)$$

where $v(\mathbf{r}_i,t_j)$ represents the EEG measurement on the ith electrode at the time t_j, $G(\mathbf{r}_i,\mathbf{l}_j)$ is a 1×3 vector describing the forward field generated by the jth dipole at the ith electrode location, and $\mathbf{s}_i(t_j)$ is 3×1 a vector describing the ith dipole moment at time t_j. The above equation can be written in matrix notation as

$$\underset{m\times n}{\mathbf{v}(t)} = \underset{m\times 3p}{\mathbf{G}}\,\underset{3p\times n}{\mathbf{S}(t)}\,. \quad (2)$$

The original MUSIC algorithm assumes the rank of the signal subspace is equal to the number of dipoles and each of these dipoles has a linearly independent time course. This definition of source arbitrarily precludes synchronous sources in the brain. To enable the search for synchronous sources the IT source model was proposed in R-MUSIC. In this model, a "source" is not represented by a single dipole but an IT, which is comprised of one or more nonrotating dipoles with perfectly correlated time courses. Each IT has a time course that is independent of other ITs, so the rank of the signal subspace is equal to the number of ITs rather than the number of dipoles. Within this framework, the p dipoles in (1) can be grouped into r subsets, each representing an IT. Therefore, (2) can be rewritten as

$$\underset{m\times n}{\mathbf{v}(t)} = \begin{bmatrix}\mathbf{G}(\boldsymbol{\rho}_1) & \cdots & \mathbf{G}(\boldsymbol{\rho}_r)\end{bmatrix}\mathbf{S}(t) = \underset{m\times r}{\mathbf{G}(\boldsymbol{\rho})}\,\underset{r\times n}{\mathbf{S}(t)} \quad (3)$$

where $\boldsymbol{\rho}_i \equiv [\mathbf{l}_1^{(i)},\cdots,\mathbf{l}_{p_i}^{(i)}]$ represents the location parameters of p_i dipoles contained in the ith IT.

If the dipole orientations are factored out from the moments then (3) can be reduced to [10]

$$\begin{aligned}\mathbf{v}(t) &= \mathbf{G}(\boldsymbol{\rho})\mathbf{S}(t) = \mathbf{G}(\boldsymbol{\rho})[\mathbf{u}_1 \quad \cdots \quad \mathbf{u}_r]\begin{bmatrix} m_1(t) \\ \vdots \\ m_r(t)\end{bmatrix} \\ &= [\mathbf{a}(\boldsymbol{\rho}_1,\mathbf{u}_1) \quad \cdots \quad \mathbf{a}(\boldsymbol{\rho}_r,\mathbf{u}_r)]\begin{bmatrix} m_1(t) \\ \vdots \\ m_r(t)\end{bmatrix} \\ &= \mathbf{A}(\boldsymbol{\rho},\mathbf{u})\mathbf{M}(t) \end{aligned} \quad (4)$$

where $\mathbf{u} = [\mathbf{u}_1,\cdots,\mathbf{u}_r]$ are the unit-norm generalized orientation vectors for the r ITs. The orientation vectors are generalized to include the orientation of all dipoles in an IT.

When additive noise is considered, (4) become

$$\mathbf{v}(t) = \mathbf{A}\mathbf{M}(t) + \mathbf{N}(t) \tag{5}$$

If the noise is assumed to be white with zero mean, then the autocorrelation of the measurement is

$$\mathbf{R_V} = E\{\mathbf{v}\mathbf{v}^T\} = \mathbf{A}\left(E\{\mathbf{M}\mathbf{M}^T\}\right)\mathbf{A}^T + n\sigma_e^2\mathbf{I} \tag{6}$$

where $E\{\cdot\}$ is the expectation operator, σ_{e}^2 is the variance of the noise and $\mathbf{I}$ is the identity matrix. The autocorrelation matrix $\mathbf{R_V}$ can be partitioned into signal subspace and noise subspace as follows:

$$\begin{aligned}\mathbf{R_V} &= [\Phi_s, \Phi_e]\begin{bmatrix}\Lambda + n\sigma_e^2\mathbf{I} & 0\\ 0 & n\sigma_e^2\mathbf{I}\end{bmatrix}[\Phi_s, \Phi_e]^T\\ &= \Phi_s\left(\Lambda + n\sigma_e^2\right)\Phi_s^T + \Phi_e\left(n\sigma_e^2\right)\Phi_e^T\\ &= \Phi_s\Lambda_s\Phi_s^T + \Phi_e\Lambda_e\Phi_e^T\end{aligned} \tag{7}$$

where Λ are r signal eigenvalues, Λ_s contains r estimated signal eigenvalues, and Λ_{e} is a matrix of $(m-r)$ noise-only eigenvalues. The signal subspace is defined as span (Φ_{s}), and the orthogonal or noise-only subspace is defined as span (Φ_{e}). The columns of $\mathbf{A}(\boldsymbol{\rho}, \mathbf{u})$ should span the same subspace as Φ_{s}. By projecting ITs which contain one or multiple columns of $\mathbf{A}(\boldsymbol{\rho}, \mathbf{u})$ into the signal subspace, the best fitting ITs can be determined. This forms the basis of signal subspace methods for parameter estimation of the IT model.

RAP-MUSIC is an algorithm that also recursively searches the ITs according to subspace correlation. The main feature of RAP-MUSIC is that once an IT is found its component is removed from the signal; thus, the following search is performed in the orthogonal subspace of the already-found ITs. The modified subspaces are formed by applying an orthogonal projector to both the measured field and source subspace.

For each iteration, R-MUSIC and RAP-MUSIC first scan for single dipole ITs. If no single dipole is sufficiently correlated to the modified signal subspace, then ITs consisting of two synchronous dipoles are scanned, and so forth. The original description of R-MUSIC suggested a fixed correlation threshold of 0.95 for multisource ITs. In our previous study, it was found this threshold is applicable only for a restricted range of SNR [18]. An appropriate correlation threshold is highly dependent on both the SNR and the configuration of synchronous and independent sources. A theoretical relationship between the expected model correlation and the SNR may be derived from the standard statistical interpretation of the coefficient of determination, as follows:

$$\begin{aligned}cc^2 &= \frac{\|\mathbf{GS}\|^2}{\|\mathbf{GS}+\mathbf{n}\|^2} = \frac{\|\mathbf{GS}\|^2}{\|\mathbf{GS}\|^2 + \|\mathbf{n}\|^2} = \frac{\mathrm{SNR}^2}{\mathrm{SNR}^2+1} \Rightarrow\\ cc &= \sqrt{\frac{\mathrm{SNR}_{\mathrm{est}}^2}{\mathrm{SNR}_{\mathrm{est}}^2+1}}\end{aligned} \tag{8}$$

where $\mathrm{SNR}_{\mathrm{est}}$ is based on estimates of the signal norm and noise norm. Equation (8) indicates that when SNR is low, a lower correlation threshold may be required.

However, in practice, estimating the SNR is not straightforward; hence, it is difficult to decide on a threshold. Furthermore, the best threshold also depends on the source configuration, which is, of course, unknown in most applications. When the threshold is too low, R-MUSIC and RAP-MUSIC will fail to identify synchronous sources; instead a single independent source will be found somewhere between the synchronous sources. When the threshold is too high, independent sources will be rejected and spurious synchronous sources will appear.

B. POP-MUSIC

To improve the reconstruction of synchronous sources, we propose to integrate RAP-MUSIC with the spatial-only inverse algorithm WMN. Since the wide point spread function of WMN will cause overlap of sources, we first reduce the candidate source space. With a reduced source space, the inverse problem becomes less underdetermined,and, thus, the inverse solution can be more robust to noise. The method of reducing source space is described as follows.

Suppose the rank of the estimated signal subspace is r. RAP-MUSIC will then iteratively search for r ITs. After each IT is found, RAP-MUSIC removes the signal component associated with this IT by applying an orthogonal projector $\Pi_{\mathrm{i}}^{\perp}$ to both the measured field and present source subspaces and continues searching in the projected space. For the Ith iteration the projector $\Pi_{\mathrm{i}}^{\perp}$ is defined as

$$\Pi_i^{\perp} \equiv \left(\mathbf{I} - \hat{\mathbf{A}}_i\left(\hat{\mathbf{A}}_i^T\hat{\mathbf{A}}_i\right)^{-1}\hat{\mathbf{A}}_i^T\right) \tag{9}$$

where $\hat{\mathbf{A}}_i$ represents the IT model that has been found by previous iterations.

We can denote the ith independent component of the signal as $\mathbf{X}i$. If the correlation between the ith IT and $\mathbf{X}i$ is perfect, i.e. unity, then $\Pi_i^{\perp}\mathbf{X}i = 0$. This means that in the projected space, the signal component $\mathbf{X}i$ has been removed. RAP-MUSIC will stop searching when r ITs are found. It is assumed that these r ITs can represent the signal, so searching for more ITs will merely fit additional sources to noise. This is true only if the r ITs can precisely fit the signal, i.e., in each iteration i, $\Pi_i{}^{\perp}\mathbf{X}i = 0$ holds.

RAP-MUSIC scans for single dipoles first, so when synchronous sources are present, a single independent source is first found as the global maxima. A search for multiple synchronous sources is initiated only if the correlation of this source is lower than some threshold. If an independent source is mistakenly found in place of multiple synchronous sources, i.e., $\hat{\mathbf{A}}_i$ is not composed of the true sources responsible for $\mathbf{X}i$, then $\Pi_i^{\perp}\mathbf{X}i \neq 0$. This means the signal component $\mathbf{X}i$ is not completely removed by projecting the signal subspace to $\Pi_{\mathrm{i}}^{\perp}$ and there will be some unexplained "residual" of $\mathbf{X}i$ in the transformed signal space.

Thus, if the searching process is continued after r ITs are found, RAP-MUSIC will locate sources that are partially associated with noise and partially associated with the residual signal components $\Pi_i^{\perp}\mathbf{X}i$. Such residual signal components are likely to be localized at the true positions of synchronous sources as these positions are highly correlated to the residual.

Based on this reasoning, we modified the RAP-MUSIC process to search for k single-dipole ITs, where k is a number

considerably larger than r. In our study, we set k to the full rank of the measurements, including noise components. Therefore, among these k single dipole ITs, some are associated with real independent sources; some are associated with synchronous sources, and others are associated with noise. These k locations are a small portion of the source space in the whole head volume but are likely to contain the true independent and synchronous source locations when the number of these sources is less than k. In order to increase the possibility of retaining all true source locations in the search space, we expand the candidate source space by including the neighboring nodes of the k locations described above. This inclusion of neighboring nodes ensures that the inverse problem remains underdetermined. The modified source space, thus, has q sources ($q > m/3$), where m is the number of EEG sensors. The validity of this method of reducing source space was tested by statistical studies on simulated data. The details of the simulated study are reported in the "Results" section of this paper.

Even in this reduced source space, exhaustive searching for synchronous sources using RAP-MUSIC is difficult. Suppose the source space has been reduced from several thousand to 200, exhaustive searching for four synchronous sources still involves millions of combinations. Here we introduce an alternative way to recover synchronous sources to avoid this multidimensional searching.

We employ the WMN method over the reduced candidate source space to roughly estimate the source locations and waveforms. As stated above, spatial-only methods such as WMN are not sensitive to source correlation and, thus, the synchrony between sources can be reflected to some degree in the reconstructed waveforms. A correlation analysis is then performed on the reconstructed sources. The sources are first sorted according to their power. For a given source S_a, we search for the N largest sources whose correlations with S_a exceed a threshold. These N sources and the source S_a are then saved as a "correlated group." Here, we encounter a threshold problem as in RAP-MUSIC. This threshold states how large a correlation is required if a source is considered to be synchronized to S_a. It should be noted that this correlation threshold is distinctly different from that in RAP-MUSIC. First, the correlation here is not "subspace correlation" but correlation coefficient between two waveforms. Second, this correlation threshold plays a different role than the correlation threshold in RAP-MUSIC. This threshold decides "which sources are possible synchronous companions to S_a" rather than "do we need any additional synchronous sources in order to adequately explain the current subspace signal component." In other words, our threshold only affects the selection of a grouping of source sites, but does not trigger a multidimensional search. In this algorithm, less significant sources are excluded by sorting the possible synchronous companions of S_a by their power. Because of this, it is safe to set a conservatively low threshold in order to favor the detection of synchronous companions. This is a strategy that would not work for RAP-MUSIC. We, therefore, gradually reduce the threshold until N companions are found in each group, where N is a parameter selected by the user.

The source space is, thus, divided into several "correlated groups." Each one of the q "correlated groups" is then taken as a candidate IT. The RAP-MUSIC algorithm is then applied again to search for r ITs from among these predetermined groups. This means that when a dipole is scanned, its correlated companions are automatically included. On the other hand, because a "correlated group" contains multiple sources, some spurious sources may appear in the final result. Fortunately, the spurious sources are usually weak compared to the true sources. Based on the model parameters found by RAP-MUSIC, the waveform of the sources can be estimated using various optimization standards, such as least-squares (as in R-MUSIC and RAP-MUSIC), WMN, or other methods. In our study, we have used least square.

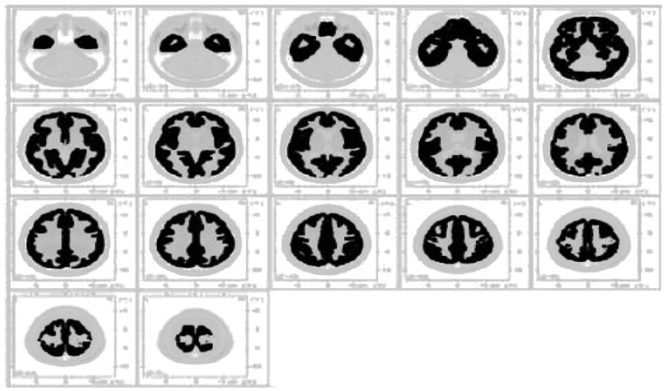

Fig. 1. Topography of the spherical head model. The upper-left slice is the lowest part of the brain; the lower-right slice is the topmost part of the brain. The dark part is the solution space of the inverse problem.

In summary, the POP-MUSIC algorithm can be stated as follows.

1) Iteratively search for k single-source ITs using RAP-MUSIC, where k is the rank of measurement. Find the neighbors of these k source locations.
2) Reduce the source space to the source set found by Step 1), including the neighbors. Estimate the source waveform for each source in this space by applying WMN at each time sample.
3) For each source, find the N largest correlated companions, thus forming a collection of "correlated groups," excluding nearest neighbors.
4) Perform RAP-MUSIC to find r ITs from these correlated groups.
5) Calculate the inverse using the model parameters derived in Step 4).

III. Results

We evaluated the performance of this POP-MUSIC algorithm using both simulated data and clinical data. For the simulated data, we employed a three-shell spherical head model [19] registered to the Talairach human brain atlas [20]. The solution space was restricted to cortical gray matter and hippocampus, consisting of 2394 nodes at a $7 \times 7 \times 7$ mm spatial resolution. Fig. 1 shows the solution space (dark area) along 17 axial slices through the brain. The measurement space consisted of 127 electrodes on the scalp. We employed this spherical head model in our simulations because this model has been widely

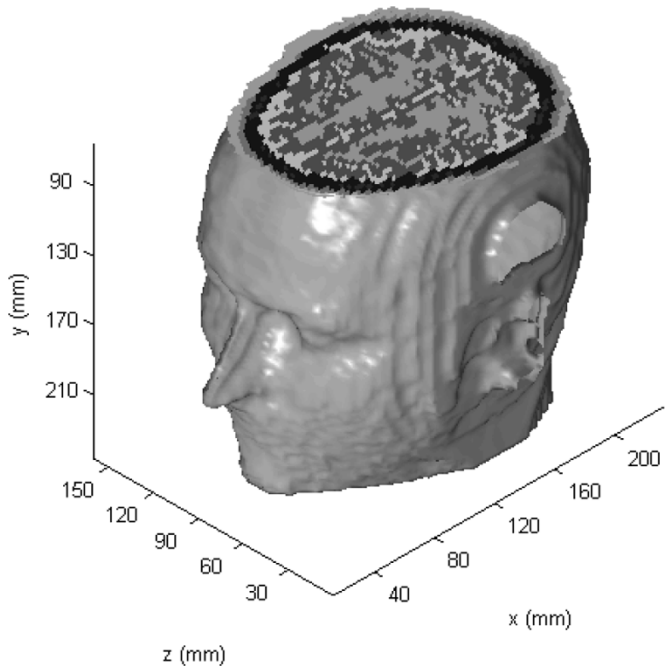

Fig. 2. Realistic-geometry head model and the coordinate system, with cutaway illustrating classified tissues.

used in other studies [14], [21], [22] so our results can be compared with those. For the clinical data analysis we used a realistic-geometry head model based on classified magnetic resonance images of a human head [23]. The lead-field matrix was calculated using the finite element method [24]. This model and the associated coordinate system are illustrated in Fig. 2. The source space consisted of 3 035 locations sampled from the cortical surface at a resolution of $4 \times 4 \times 4.25$ mm. Our clinical data used a 21-channel EEG, so the lead-field matrix had a dimension of 21×9105.

A. Simulation Study

A statistical study was first conducted to verify our method of trimming the source space. We simulated 7 dipole sources on randomly selected locations both in the realistic and the spherical head model. Among these 7 dipoles, 3 were independent and the other 4 were synchronous. The candidate source space was then searched as described in Section II-B. The simulation was repeated 100 times. Our statistical results showed that in the realistic head model the source space was reduced from 3035 voxels to 218 voxels on average. In the spherical model, the source space was reduced from 2394 voxels to 257 voxels. Within the reduced source space, all of the independent sources and 69% of the synchronous sources were faithfully retained for the realistic head model, while all independent sources and 77% of the synchronous sources were retained for the spherical model. For the lost synchronous sources, their closest neighbors within the reduced source space had an average distance of 6.3 mm (realistic model) and 17.4 mm (spherical model) from the true locations, which are both about 2 grid positions in the sampled source spaces. This result shows that our method can efficiently reduce the sources space while retaining the voxels that are associated with the true sources.

In order to compare the performance of POP-MUSIC and RAP-MUSIC in localizing synchronous sources, we began with some simple synchronous source configurations. Two 100% correlated sources with random orientations were placed in the 10th slice of our spherical head model. One source was located in the left occipital area and the other in the right occipito-temporal area, as shown in Fig. 3(a). Here, the activities of the sources are superimposed on the MR images. The power of the source is illustrated using a grey scale where dark is maximum and light is minimum. Note that in order to show single dipole sources more clearly on the MR images, we have drawn a circle at each dipole location so that a source can appear bigger on the image. For simplicity, a sinusoidal waveform of 10 Hz was taken as the source waveform to emulate alpha activity in these areas. The magnitude of the left source is 0.7 that of the right sources. The simulated source waves were 2 s in length with a sampling frequency of 100 Hz.

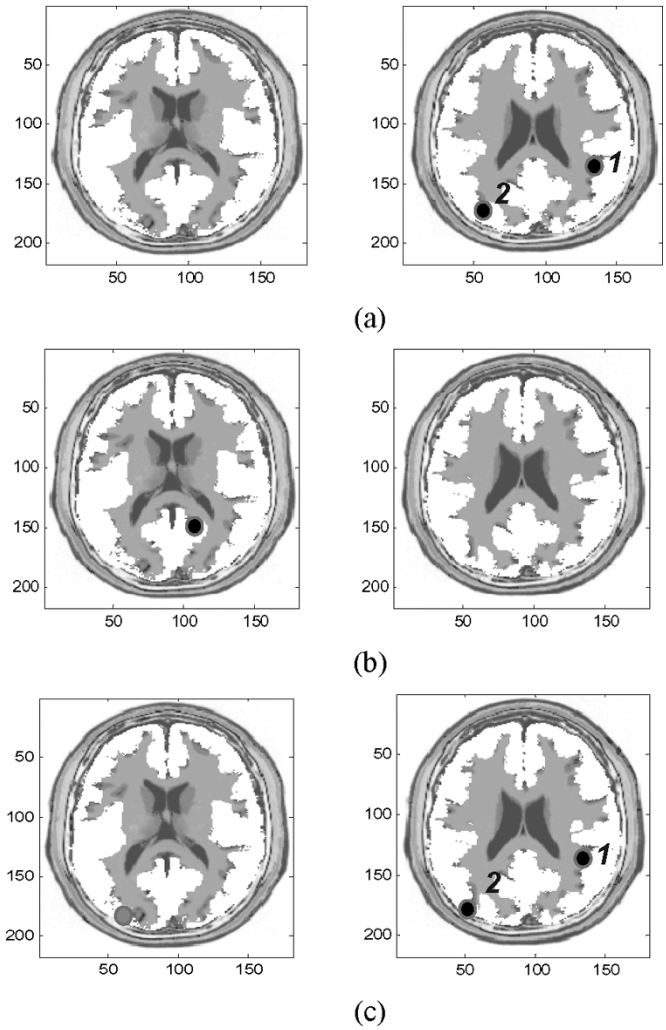

Fig. 3. Reconstruction of two synchronous sources. (a) The simulated source configuration; (b) solution of RAP-MUSIC algorithm; (c) solution of POP-MUSIC algorithm.

The simulated measurement was acquired through forward calculation using the spherical head model discussed above. White noise was then added to the simulated measurement to produce an SNR of 15 db. The SNR was defined as

$$\mathrm{SNR} = 20 \log_{10} \left(\frac{F(\mathbf{v_{exact}})}{F(\mathbf{e})} \right) \tag{10}$$

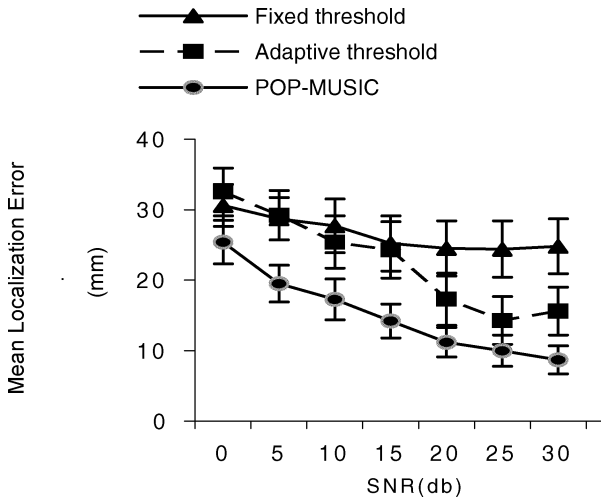

Fig. 4. Localization errors for one independent and two synchronous sources at different noise levels. The sources are randomly placed and the distance between two synchronous sources is fixed to 80 mm. The two curves on the top are produced by RAP-MUSIC using two different threshold strategies. The curve on the bottom is produced by POP-MUSIC.

where $F(\mathbf{v_{exact}})$ is the Frobenius norm of the simulated noise-free observations, and $F(\mathbf{e})$ is the Frobenius norm of the added noise $\mathbf{e}$, which was independent and identically distributed on each channel.

We first employed RAP-MUSIC with a fixed threshold of 0.95 as suggested in [10]. RAP-MUSIC ended the search with a single dipole which is located approximately in the middle of the two simulated sources but in the adjacent slice [Fig. 3(b)]. This single dipole IT had a correlation of 0.9971 with the estimated signal subspace. This result shows that a fixed threshold of 0.95 is insufficient for recovering the synchronous sources in this head model. We next applied POP-MUSIC to the same data with a correlated group size of $N = 4$, and a correlation threshold of 0.8. POP-MUSIC reconstructed three synchronous sources as shown in Fig. 3(c). Two sources were located in the correct slice with very small localization error. The third source was in the adjacent slice but still very close to the original source location. The waveforms of these 3 sources were all highly correlated to the simulated sinusoid wave with correlation coefficients larger than 0.99. This result shows that POP-MUSIC is able to reflect the synchrony between these two brain areas, though some spurious nearby sources may occur.

In order to gain some quantitative information about the performance of these two algorithms, the following statistical study was conducted. We placed one independent source and two synchronous sources with random orientations at randomly selected locations in the head model. The distance between two synchronous sources was fixed at 80 mm. White noise was then added to the simulated measurements. We evaluated these two algorithms at different noise levels by increasing the SNR from 0 to 30 dB in 5-dB increments. For each SNR, 100 randomized source configurations were generated and the inverse calculations were performed by RAP-MUSIC and POP-MUSIC respectively. Here, we tried two different threshold strategies for RAP-MUSIC. First the correlation threshold was set to 0.95 as proposed in [10], and then an SNR related threshold was used [18]. The parameters for POP-MUSIC were the same as described in the previous simulation. Fig. 4 shows the mean value of localization errors for these two algorithms. Vertical bars indicate the 95% confidence interval on the mean. In this study, localization error is defined as the average distance between the simulated and reconstructed source in the best of the possible two-way matches between actual and reconstructed sources. In cases where RAP-MUSIC reconstructed two synchronous sources as a single source, we defined the localization error as the average distance from the reconstructed source to each of the two actual sources. This did not occur with POP-MUSIC, because it always reconstructs more than the actual number of sources. It should be noted that this definition of localization error does not capture the effect of spurious sources that may be produced by POP-MUSIC.

Though the adaptive threshold strategy slightly improves the localization ability of RAP-MUSIC, it still has large localization error, especially when SNR is low, because the search for two synchronous sources often ends up with a single source. Compared to RAP-MUSIC, POP-MUSIC has better performance in recovering the simulated sources. When the SNR is 15 db, the average localization error is about 14.2 mm, which is slightly more than 2 grid points.

In the following study, we simulated six sources in the brain. The locations of these sources are displayed in Fig. 5(a). Among them one source in the frontal lobe has a temporal waveform oscillating at 15 Hz (source1); the other five sources in the occipital and temporal lobes have completely synchronous activities at 9 Hz (source2-source6). These six sources have same magnitude. White noise was added to the simulated measurement to achieve an SNR of 20 dB. We first applied RAP-MUSIC using the fixed correlation threshold of 0.95. It correctly located the independent source (source1) with a subspace correlation of 0.9983, but the synchronous sources were not fully recovered and only a single source was found near source6 with a very high subspace correlation of 0.9901. The reconstructed sources are shown in Fig. 5(b). In order to enable a search for the synchronous sources, we increased the correlation threshold to 0.9950. Two synchronous sources (source6 and source3) were then found with relatively small localization errors [Fig. 5(c)]. This two-source IT had a correlation of 0.9964 with the signal subspace. This means that if we want to obtain more than two synchronous sources, a threshold larger than 0.9964 would be required.

We next applied POP-MUSIC to this simulated data with a correlated group size of $N = 10$, and a correlation threshold of 0.8. Fig. 5(d) shows the source locations scanned by POP-MUSIC. Although this source image is not exactly the same as Fig. 5(a), all of the simulated sources were recovered with rather small localization error. Note again that some small spurious sources have appeared because POP-MUSIC combines multiple synchronous sources to make an IT. However, these spurious sources are very weak, or are close to the real source. This shows that POP-MUSIC is able to recover complex source configurations containing multiple independent and synchronous sources.

B. Localization of Epileptiform Activity

In this section, we employ RAP-MUSIC and POP-MUSIC to localize epileptiform activity. A seizure focus is a group of neu-

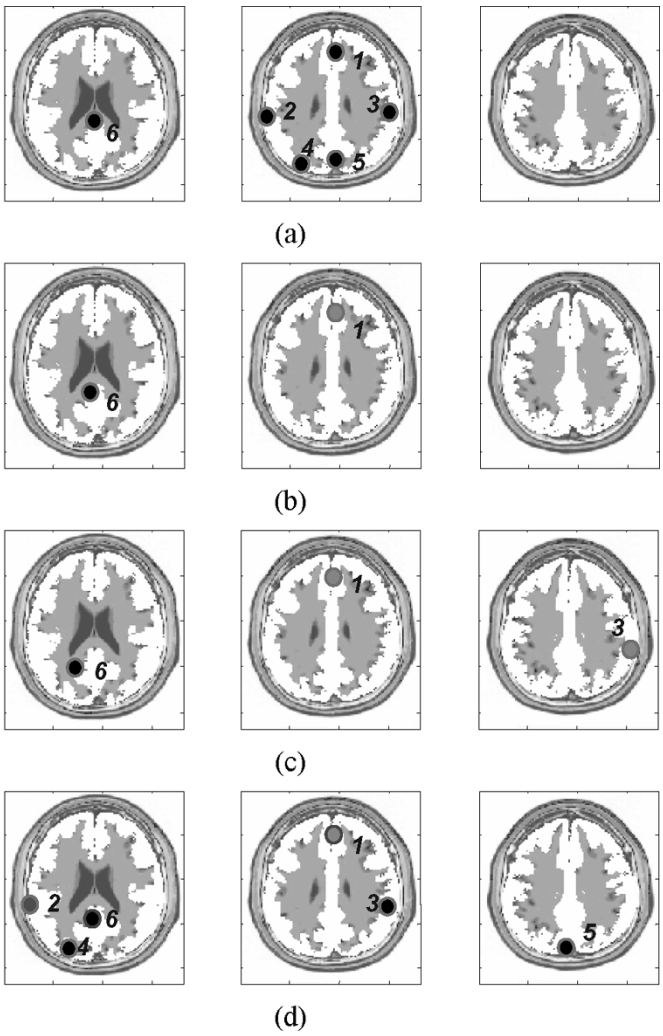

Fig. 5. Reconstruction of complex source configurations. (a) The simulated source locations. Source1 is independent to the other 5 sources, those are completely synchronous. (b) Reconstructed source configuration by RAP-MUSIC with a correlation threshold of 0.95 (c) Reconstructed source configuration by RAP-MUSIC with a threshold of 0.995 (d) The sources reconstructed by POP-MUSIC.

rons that trigger the abnormal discharge of the brain and cause the seizure. Localization of the foci is very important in the surgical treatment of epilepsy. In this study, we analyzed the clinical EEG data of an epileptic patient suffering from frontal lobe partial epilepsy. Informed consent was obtained from the patient. A 21-channel scalp EEG was acquired using the extended 1020 international layout, digitized at 256 Hz and bandpass filtered at 0.5–40 Hz. We applied the realistic geometry head model described above to this data. It should be noted that this realistic head model was not based on the head of the patient.

The foci were first determined by a physician based on subdural EEG recordings. Intracerebral electrodes with multiple contacts were implanted in the frontal and adjacent lobes, where the location of epileptogenic foci were suspected. One subdural grid with 8×4 contacts and four subdural strips with 8 contacts were used. The post-implantation location of the electrodes can be seen in the X-Ray image (Fig. 6). The locations of the foci determined by the physician are shown in Fig. 6 as white crosses. The frequency of seizure has been substantially reduced since the surgery.

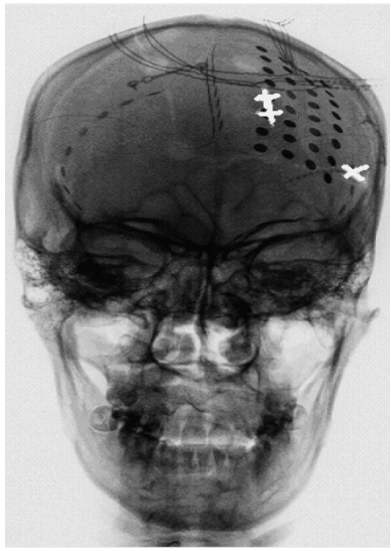

Fig. 6. X-ray image of the intracerebral electrodes. The white crosses indicate the locations of epileptic foci.

In an attempt to localize the seizure foci using scalp EEG, a 0.5-s data segment containing an interictal spike and wave complex was inverted. This complex wave appeared 10 s prior to seizure onset. Epileptic seizures are suggested to be caused by hyper-synchronization of the neurons so significant synchronization may exist during the generation and propagation of the epileptiform waves. RAP-MUSIC was first applied to this 0.5-s data with the reconstructed dipole locations (dark circles) superimposed on the MR images in Fig. 7(a)–(d). There are 41 sagittal MR images associated with the head model but here we show only the slices where sources are located. The z coordinates (refer to Fig. 2) of the slices are also shown in these images. Among the four reconstructed sources, one source is close to the midbrain [Fig. 7(a)] and the other three sources are all in the right hemisphere. These sources do not agree with the foci locations determined by the physician. This demonstrates that when synchronous sources are not appropriately processed, the reconstructed source configuration could be far from the truth.

POP-MUSIC was then applied to the same 0.5-s data segment. The correlated group size N is set to 6 and the correlation threshold was set to 0.85. Fig. 7(e)–(h) shows the reconstructed source locations. The dipoles shown in Fig. 7(e)–(g) are in the left frontal lobe and are close to the foci shown in Fig. 6. POP-MUSIC also found a source in the deep structure of the cortex near the corpus callosum and thalamus [Fig. 7(h)]. This source may reflect the synchronization between cortex and thalamus which is reported to play an important role in seizure propagation [25]. It should be noted that our experimental data consists of only 21 EEG channels, and the accuracy of source localization is usually questionable with so few sensors. In [26], Mosher *et al.* determined the error bound of EEG source localization for different sensor configurations. Their results show that when the sensors are as few as 21, the average RMS lower bound can be several centimeters. This may explain why RAP-MUSIC produces inconsistent results on these data. However, this limited preliminary study provides some qualitative evidence that POP-MUSIC is applicable to real (as opposed to simulated)

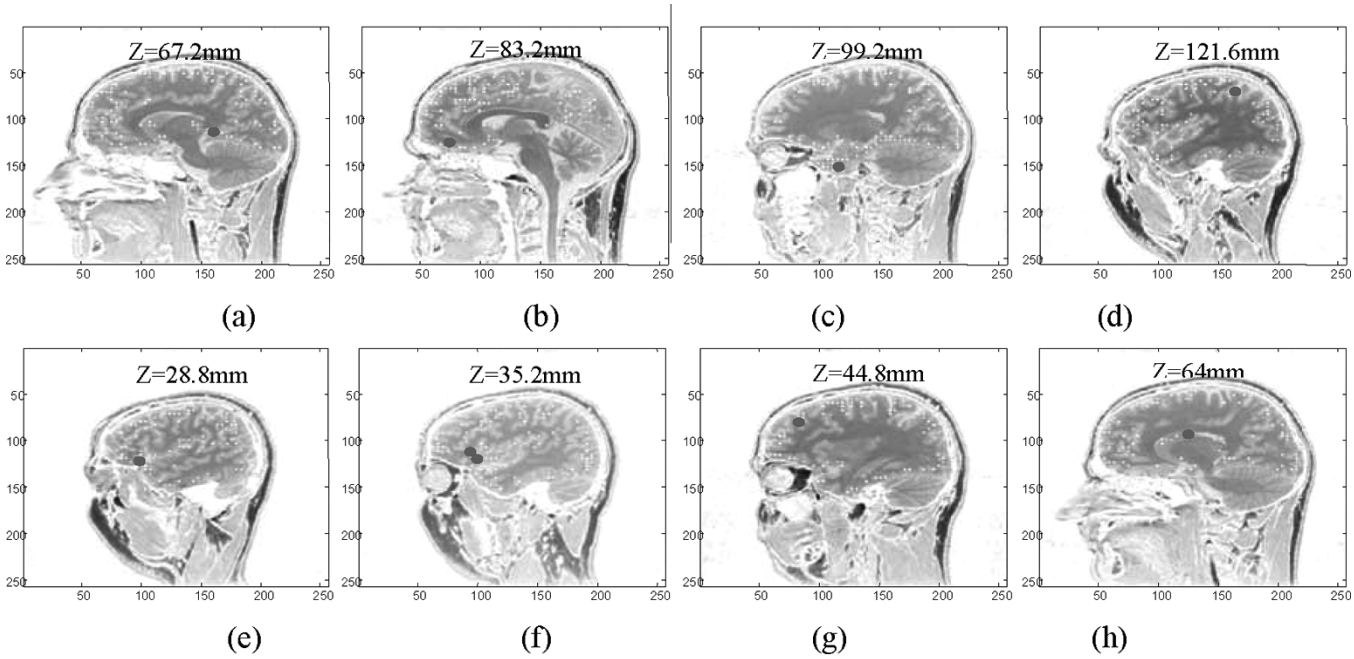

Fig. 7. Seizure sources reconstructed by RAP-MUSIC are shown in (a)–(d). Most of them are located in the right hemisphere and are inconsistent with the true foci locations. Sources reconstructed by POP-MUSIC are shown in (e)–(g). They are close to the true foci locations.

data, and may have some advantage over RAP-MUSIC in situations where substantial synchronous activity can be expected.

IV. Discussion

As synchrony is an important mechanism in brain functioning, an inverse method that can recover the highly correlated activity is desirable. In this paper, we present a method which takes advantage of the spatio-temporal source model employed by R-MUSIC and RAP-MUSIC, but avoids the exhaustive searching for synchronous sources among numerous possible combinations of dipoles. This algorithm combines spatial-only and spatio-temporal approaches in a hybrid way. Recent development in brain mapping techniques has proven the efficiency of such combining strategies. In [27], Dale *et al.* proposed an approach which employs the solution of the MUSIC algorithm as a weighting matrix in the minimum norm reconstruction. We also have implemented a combining strategy in our recently developed algorithm SSLOFO [22]. Here, our hybrid algorithm focuses on the highly correlated activities in the brain. For an EEG data segment, RAP-MUSIC can robustly reveal independent sources and reconstruct the source waveforms, while the spatial-only method WMN is able to reflect the correlated activities among brain regions. Our effort is to seek a combination of these two methods in a way that preserves the desirable features of each.

We reduce the smoothing effect of WMN by first trimming the candidate source space. The source waveforms reconstructed by WMN are then analyzed and correlated sources are grouped together. Note that when the data contains noise, the technique of regularization should be applied in the WMN algorithm. We employed Tikhonov-Phillips regularization [28] in our study. Other low-resolution methods based on the minimum norm algorithm are possible alternatives to WMN. Algorithms such as LORETA and sLORETA can also roughly reveal the energy distribution but usually produce smoother maps. In a smooth reconstruction, the sources will appear to be overly correlated, so the correlation threshold for source grouping may need to be adjusted in that case. It should be pointed out that this correlation threshold is also related to SNR. However, this threshold can be underestimated because its only function is to exclude the most asynchronous sources. The correlated sources are sorted by power and subjected to another RAP-MUSIC scan.

A parameter that should be emphasized is N, the number of synchronous companions in each group. This number indicates how many synchronous sources are included in a group and is application-specific. A large group may produce some spurious sources and a small group may cause loss of some synchronous sources. However, a larger N is usually safer because although N synchronous sources are included, some of their final energies will be small. We repeated the simulation in Fig. 3 using different choices of N. The sources reconstructed by POP-MUSIC are shown in Fig. 8. It can be seen that an increasing N may result in more spurious sources. However, when N increases from 8 to 11, there is no significant change in the number of spurious sources because the number of the synchronous companions in a group is also limited by the correlation threshold. An automated strategy for determining N may be to start small and iteratively apply POP-MUSIC until the residual signal falls below an estimate of the noise. We have not yet investigated this strategy.

POP-MUSIC recovers synchronous sources with the price of producing some small spurious sources synchronized to independent sources. Theoretically, it is possible to employ a very high threshold to enable the search for multiple synchronous sources using RAP-MUSIC. Such a strategy will reject independent sources and will also produce spurious synchronous

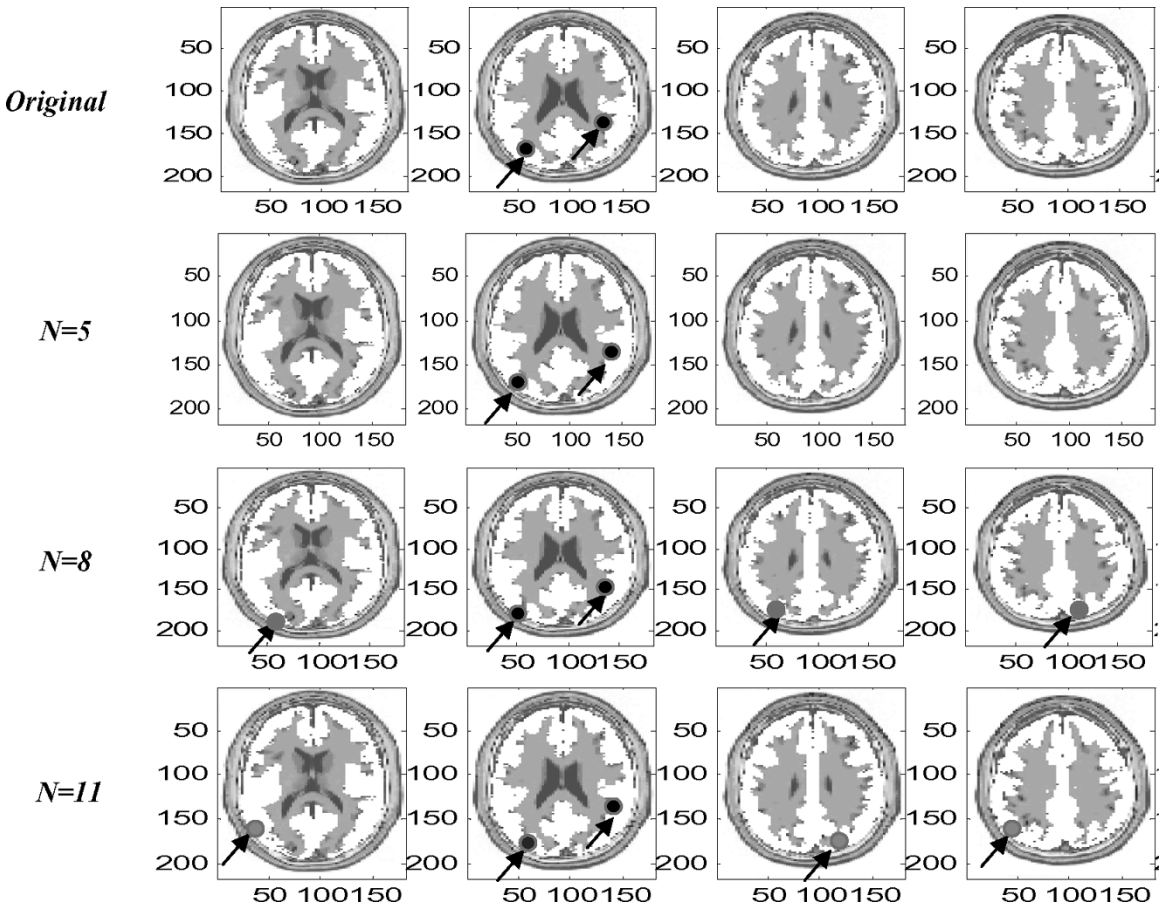

Fig. 8. Reconstruction of two synchronous sources with different choices of N.

sources. However, the resulting multidimensional search is impractical and a suitable threshold is still not easy to choose. Note that because of the ill-posed nature of the inverse problem, spurious sources are unavoidable in most imaging inverse algorithms. By trimming the candidate solution space, POP-MUSIC has greatly reduced the influence of spurious sources.

It should be emphasized that the inverse problem has no unique solution and every algorithm has its own appropriate application. When synchronous activity may not be significant or spurious sources are to be avoided, methods such as R-MUSIC and RAP-MUSIC may be favorable. When correlated activities are significant and the interaction among different brain regions are to be investigated, POP-MUSIC may be favorable.

V. Conclusion

Simulated data and experimental data have been employed to test the performance of POP-MUSIC. Results on simulated data demonstrated that POP-MUSIC has some potential advantages in handling synchronous sources. When applied to the epileptic scalp EEG, POP-MUSIC localized sources which are close to the true foci as determined by a physician from implanted electrodes, and revealed some activity in the deep brain structure that may participate in a thalamo-cortical circuit. These preliminary studies indicate POP-MUSIC has potential in neural synchrony analysis of brain function.

Acknowledgment

The authors would like to thank Dr. R. D. Pascual-Marqui, J. Haueisen, and Dr. G. Zhang for providing the head models and clinical data.

References

[1] A. K. Engel, P. Fries, and W. Singer, "Dynamic predictions: oscillations and synchrony in top-down processing," *Nat. Rev. Neurosci.*, vol. 2, pp. 704–716, 2001.

[2] W. H. Miltner, C. Braun, M. Arnold, H. Witte, and E. Taub, "Coherence of gamma-band EEG activity as a basis for associative learning," *Nature*, vol. 397, pp. 434–436, 1999.

[3] R. Blake and Y. Yang, "Spatia and tempora coherence in perceptual binding," *Proc. Nat. Acad. Sci. USA*, vol. 94, no. 13, pp. 7115–7119, 1997.

[4] E. Salinas and T. Sejnowski, "Correlated neuronal activity and the flow of neural information," *Nat. Rev. Neurosci.*, vol. 2, pp. 539–550, 2001.

[5] F. Varela, J. Lachaux, E. Rodriguez, and J. Martineri, "The brain web: phase synchronization and large-scale integration," *Nat. Rev. Neurosci.*, vol. 2, pp. 229–239, 2001.

[6] J. Fell, P. Klaver, K. Lehnertz, T. Grunwald, C. Schaller, C. Elger, and G. Fernández, "Human memory formation is accompanied by rhinal-hippocampal coupling and decoupling," *Nat. Neurosci.*, vol. 4, pp. 1259–1264, 2001.

[7] J. Gross, J. Kujala, M. Hamalainen, L. Timmermann, A. Schintzler, and R. Salmelin, "Dynamic imaging of coherent sources: studying neural interactions in human brain," *Proc. Nat. Acad. Sci. USA*, vol. 98, no. 2, pp. 694–699, 2001.

[8] S. Baillet, J. C. Mosher, and R. M. Leahy, "Electromagnetic brain mapping," *IEEE Signal Process. Mag*, vol. 18, no. 6, pp. 14–30, Nov. 2001.

[9] C. M. Michel, M. M. Murray, G. Lantza, S. Gonzalez, L. Spinelli, and R. Grave de Peralta, "Brain source image," *Clin. Neurophysiol.*, vol. 115, no. 10, pp. 2195–2222, 2004.

[10] J. C. Mosher and R. M. Leahy, "Recursive MUSIC: a framework for EEG and MEG source localization," *IEEE Trans. Biomed. Eng.*, vol. 45, no. 11, pp. 1342–1354, Nov. 1998.
[11] ——, "Source localization using recursively applied and projected (RAP) MUSIC," *IEEE Trans. Signal. Process.*, vol. 47, no. 2, pp. 332–340, Feb. 1999.
[12] M. S. Hämäläinen, "Magnetoencephalography—theory, instrumentation, and applications to noninvasive studies of the working human brain," *Rev. Mod. Phys.*, vol. 65, pp. 413–497, 1993.
[13] R. D. Pascual-Marqui, C. M. Michel, and D. Lehmann, "Low resolution electromagnetic tomography: a new method for localizing electrical activity in the brain," *Int. J. Psychophysiol.*, vol. 18, pp. 49–65, 1994.
[14] R. D. Pascual-Marqui, "Review of methods for solving the EEG inverse problem," *Int. J. Bioelectromag.*, vol. 1, pp. 75–86, 1999.
[15] ——, "Standardized low resolution brain electromagnetic tomography(sLORETA): technical details," *Meth. Findings Exp. Clin. Pharmacol.*, vol. 24D, pp. 5–12, 2002.
[16] I. F. Gorodnitsky, J. S. George, and B. D. Rao, "Neuromagnetic source imaging with FOCUSS: a recursive weighted minimum norm algorithm," *Electroenceph. Clin. Neurophysiol.*, vol. 95, pp. 231–251, 1995.
[17] M. Fuchs, M. Wagner, T. Kohler, and H. Wischmann, "Linear and nonlinear current density reconstructions," *J. Clin. Neurophysiol.*, vol. 16, no. 3, pp. 267–295, 1999.
[18] B. Kaytal and P. Schimpf, "Multiple current dipole estimation in a realistic head model using R-MUSIC," in *Proc. IEEE EMBS 26*, vol. 1, 2004, pp. 829–832.
[19] J. P. Ary, S. A. Klein, and D. H. Fender, "Location of sources of evoked scalp potentials: corrections for skull and scalp thickness," *IEEE Trans. Biomed. Eng.*, vol. BME-28, pp. 447–452, 1981.
[20] J. Talairach and P. Tournoux, *Co-Planar Stereotaxic Atlas of the Human Brain*. Stuttgart, Germany: Thieme, 1988.
[21] H. Liu, X. Gao, P. Schimpf, F. Yang, and S. Gao, "A recursive algorithm for the three-dimensional imaging of brain electric activity: shrinking LORETA-FOCUSS," *IEEE Trans. Biomed. Eng.*, vol. 51, no. 10, pp. 1794–1802, Oct. 2004.
[22] H. Liu, P. Schimpf, G. Dong, X. Gao, F. Yang, and S. Gao, "Standardized shrinking LORETA-FOCUSS (SSLOFO): a new algorithm for spatio-temporal EEG source reconstruction," IEEE Trans. Biomed. Eng., 2006, to be published.
[23] N. Shrinidhi, D. R. Haynor, Y. Wang, D. B. Joregenson, G. H. Bardy, and Y. Kim, "An efficient tissue classifier for building patient-specific finite element models from X-ray CT images," *IEEE Trans Biomed Eng*, vol. 43, no. 3, pp. 333–337, Mar. 1996.
[24] P. Schimpf, J. Haueisen, C. Ramon, and H. Nowak, "Realistic computer modeling of electric and magnetic fields of human head and torso," *Parallel Comput.*, vol. 24, pp. 1433–1460, 1998.
[25] M. Steriade and F. Amzica, "Sleep oscillations developing into seizures on corticothalamic systems," *Epilepsia*, vol. 44, no. 12, pp. 9–20, 2003.
[26] J. C. Mosher, M. Spencer, R. M. Leahy, and P. Lewis, "Error bounds for MEG and EEG source localization," *Electroencephalogr. Clin. Neurophysiol.*, vol. 86, no. 5, pp. 303–321, 1993.
[27] A. M. Dale and M. I. Sereno, "Improved localization of cortical activity by combining EEG and MEG with MRI cortical surface reconstruction: a linear approach," *J. Cognit. Neurosc.*, vol. 5, pp. 162–176, 1993.
[28] A. N. Tikhonov and V. Y. Arsenin, *Solutions of Ill-Posed Problems*. New York: Wiley, 1977.

Hesheng Liu (M'04) was born in Fukien, China, in 1975. He received the B.S. and Ph.D. degrees in biomedical engineering from Tsinghua University, Beijing, China, in 1997 and 2003, respectively.

His research interests include EEG/MEG inverse problem, brain-computer interface, epileptic seizure detection and prediction, electrical impedance tomography, and pattern recognition.

Paul H. Schimpf (S'94–M'95) received the B.S.E.E (*summa cum laude*), M.S.E.E., and Ph.D. degrees from the University of Washington, Seattle, in 1982, 1987, and 1995, respectively.

He is currently an Associate Professor in the School of Electrical Engineering and Computer Science at Washington State University where he coordinates the Informatics Program in Spokane, WA. His research interests include numerical methods for forward and inverse solutions to partial differential equations over complex heterogeneous domains.